Mechanical Engineering Advances 2025, 3(1), 1921.
https://doi.org/10.59400/mea1921

Article

A novel approach for wear assessment of plastic gears using image processing

Mahmoud G. Elkasrawi[1], Marah A. Elsiedy[2], Hesham A. Hegazi[3,4,*]

[1] Department of Mechatronics, Faculty of Engineering and Materials Science, German University in Cairo, Cairo 11835, Egypt
[2] Department of Production Engineering and Mechanical Design, Faculty of Engineering, Tanta University, Tanta 31527, Egypt
[3] Mechanical Design and Production Engineering Department, Faculty of Engineering, Cairo University, Giza 12613, Egypt
[4] Design and Production Engineering Department, Faculty of Engineering and Materials Science, German University in Cairo, Cairo 11835, Egypt
*** Corresponding author:** Hesham A. Hegazi, hesham.hegazi@guc.edu.eg

CITATION

Elkasrawi MG, Elsiedy MA, Hegazi HA. A novel approach for wear assessment of plastic gears using image processing. Mechanical Engineering Advances. 2025; 3(1): 1921.
https://doi.org/10.59400/mea1921

ARTICLE INFO

Received: 23 October 2024
Accepted: 28 November 2024
Available online: 5 December 2024

Abstract: Plastic gears offer numerous advantages, poised to increasingly supplant metal gears across various applications. Notably, they boast silent operation, resistance to corrosion, and lightweight properties which make them ideal for wind turbine systems. Moreover, the expanding array of plastic materials, including eco-plastics and their natural fibre composites, underscores the imperative for ongoing research into plastic gears and their composites. Addressing existing challenges is pivotal to fully harnessing their potential in sustainable development efforts. The wear of plastic gears is an important factor in plastic gear design and optimization. This paper primarily examines wear assessment in polypropylene (PP) gears by proposing and implementing a novel approach to measure the amount of wear on gear tooth profile using an image processing technique. By subjecting plastic gears to wear experimentation and employing direct image processing methods, the percentage of damage can be accurately evaluated. These percentages were 0.2% and 2.5% for 2 and 5 hours respectively. This underscores the boundless possibilities of integrating image processing techniques into the assessment of plastic gears, paving the way for deeper exploration and optimization of polymer materials for plastic gear manufacturing.

Keywords: plastic gears; wear assessment; image processing; testing of plastic gears; gears performance

1. Introduction

Polymer gears create a surge in the world of industry through various advantages such as lightweight, low manufacturing cost, inherent lubrication, and functioning without noise [1,2]. Introducing these traits, plastic gears excel in their equivalents; metallic gears in renewable energy systems such as wind turbine systems, solar panel tracking systems, marine renewable energy devices, and hydroelectric power plants [3]. A reduction of 9% in fuel consumption, 80% in inertia, and 70% in mass could be achieved when using plastic gears [4,5].

The failure modes of plastic gears are entirely different from metallic ones. For example, higher temperatures (reaching a melting temperature of 175 °C in polyoxymethylene for example) during operation due to higher operational load and speed could lead to deterioration of the mechanical properties of polymer gears [6]. For this reason, a study such as the one conducted by Singh et al. [7], considered determining a transition torque from the equation of surface temperature at which the wear is extremely high. Following the same way, Mao et al. [8] experimented with the

glass fiber reinforced polyacetal (POM) and neat POM to assess the type of failure mode which depends on the transition torque evaluated from surface temperature. In studies conducted by Elsiedy et al. [9,10], wear was added to the optimization problem as a type of design constraint to obtain the optimum design of polymer spur gears in terms of several teeth, modules, face width, and profile coefficients. Wear of the polymer gears was contained in several formations such as cracks, debris formation, breakage, and thermal damage as suggested by Ghazali et al. [11].

A plethora of studies in the literature have been conducted to investigate the wear of polymer gears. In the study of Tunalioglu and Torun [12], a 3D printed spur pinion made of polylactic acid (PLA) material meshed with steel gear was examined experimentally at different loads and speeds to determine the amount of wear using the coordinate measuring machine. It was shown that wear was significant at the root region because of the increased temperature due to the opposite direction of rolling and sliding of the engaging teeth. The results also demonstrated that the wear resistance of the material could be increased by the increase of strain rate and decrease of single tooth contact time. PLA pinion along with two other pinions made from polyethylene terephthalate (PETG) and Acrylonitrile Butadiene styrene (ABS) were meshed with steel gear in the study of Tunalioglu and Agca [13]. The aim was to compare the wear of the three materials by applying a theoretical wear equation. It was found that PETG gears exhibited the least wear at the same number of cycles. The wear and fatigue life of spur gears made of two different materials such as polyamide with 20% carbon fiber (machine cut) and carbon fiber reinforced polyamide (additive manufactured) were assessed in the study of Hribersek et al. [14]. The study revealed that at lower loads, machine-cut polyamide gears are expected to have cracks near the pitch point. On the other hand, in additively manufactured polyamide gears, cracks occurred at the root area. It was concluded that load levels have a significant effect on the wear rate and the surface temperature of gears. The wear coefficient was determined in the study of Muratovic et al. [15] analytically according to Verein Deutscher Ingenieure (VDI) standard and experimentally. The experiment was done by meshing steel pinion with polymer gear on a wear test rig. The average linear wear resulting from the experiment is used to calculate the wear coefficient which in turn is used in an iterative process to assess the wear depth during the progressive cycles. Hlebanja et al. [16] investigated two types of gear profiles (S and E- involute profiles). It was found that S gears behaved better than E gears as the former gave lower contact pressure, and less sliding contact, thus less frictional losses, temperature and wear. Increasing the width of the single tooth contact region of the polymer gear will reduce the load and temperature which are the main reasons for higher wear rates at this region as suggested by Imrek [17]. Other studies conducted by Mao and coworkers considered determining the wear rate of different polymer materials either composites or neat [1,18–23]. Wear of a neat material such as acetal is affected by the load. This conclusion was elucidated by Breeds et al. [24], Kukureka et al. [25], and Li et al. [26]. Reaching a higher load (critical value of 9.5 Nm) leads to a higher surface temperature, and melts the teeth and this in turn causes thermal bending. When adding glass fibre reinforcements to acetal material, the load capacity increases by approximately 50%, thus the gear will take time to wear till the end of the specified number of cycles. Three materials were introduced in the study of Singh et al. [7]; Acrylonitrile Butadiene

styrene (ABS), High-density polyethylene (HDPE), and poly acetal (POM). When experimenting with gears made of these materials for calculating the amount of wear at different torques and speeds, POM exhibited lower wear rates compared to ABS and HDPE at all specified torques due to the high wear resistivity of the POM material (bear until 9.5 Nm in dry conditions). Xu et al. [27] investigated the wear performance of two types of polyacetal gears: homopolymer and copolymer. It was concluded that the two gear types behaved in the same way in the first two phases of running in and linear, however homopolymer POM gear took more cycles than copolymer POM gears. It is worth mentioning that besides the sheer goal of replacing the metals with polymers, environmental aspects should be taken into account. Zorko et al. [28] experimented with a bio-based gear material (polyamide 6.10) with steel pinion and compared it with the neat PA66 at different load levels. PA 6.10 exhibited a lower wear rate than PA66 due to a lower coefficient of friction and temperature. Also, these bio-based materials are non-contaminated to the environment. The surface roughness of steel gears was studied in the research conducted by Johnney et al. [29] to estimate the amount of wear of the polypropylene gear (PP). It was inferred that the increased surface roughness of the mating gears escalates surface temperature, thus accelerating the wear rate of the PP gears. Cerne and Petkovsek [30] used the digital image correlation method (DIC) and edge displacement detection method (EDD) to investigate the amount of deflection and wear of the in-mesh gears. Both methods prove their reliability in detecting the wear in gear meshing. In another study conducted by Soudmand and Shelesh-Nezhad [31] image processing was used to detect the wear of gear made from neat polybutylene terephthalate (PBT) and the same material with montmorillonite (MMT) as a polymer matrix. The results indicated that PBT/MMT is better than neat PBT in performance (more life span than PBT). Temperature also affects wear when it is accompanied by an increase in load and speed [11,32,33,34]. In materials such as POM gears, wear is the most predominant type of failure followed by thermal bending at critical torques. All of the aforementioned studies have evaluated the amount of wear empirically and analytically. So, from a numerical point of view and based on the above analysis, this paper examines the wear inflicted on a polypropylene plastic gear by employing an image processing code to directly detect and compare wear with its initial condition. To obtain this data, the plastic gear undergoes wear testing, during which images of the gear tooth profile are captured. These images are subsequently processed and analyzed in MATLAB to detect and compare the evolution of gear wear over time.

2. Materials and methods

The purpose of this paper as mentioned before is to assess and evaluate the wear occurring on the gear tooth. To accomplish this evaluation, the polymer gear was subjected to wear using a specific apparatus resembling the gear's operation in machinery. This was followed by capturing gear tooth' images, and then applying a code for image processing to disclose the gear tooth profile and estimate it in comparison to its pre-wear condition.

2.1. Materials and specimens

For conducting this test, an injection molded gear made of polypropylene (PP) material was utilized as a pinion. This pinion was produced in the PRC laboratory at German University in Cairo (GUC). PP materials have lower density, low cost, and acceptable mechanical strength [27]. These cons make the PP materials suitable for many applications including gears. After manufacturing the PP pinion by injection molding machine, it was deemed suitable for testing and meshing with a steel gear. The geometrical parameters of both gears are presented in the following **Table 1**.

Table 1. Geometrical specifications of the testing gear pair.

Material	**Polymer (PP)**	**Steel (St50DIN)**
Number of teeth	20	24
Face Width (mm)	5	5
Module (mm)	3	3
Inner Diameter (mm)	15	15
Pitch Diameter (mm)	60	102
Yield Strength (N/mm^2)	35–40	259
Melting Point (°C)	160–165	1370

2.2. The testing machine

Before compel wear on the PP gear through testing, the PP gear must be placed in an environment closely matching its conventional operating conditions, in other words, the polymer gear meshed with steel gear engaging in a wear testing machine to simulate regular operations. It is worth mentioning that this machine has the option of varying centre distance (testing gears with various diameters). Over time, the polymer gear will be worn when the testing machine continuously works in dry conditions. The wear testing machine consists of a source motor which propels the entire system and transmits its power via a belt to the polymer gear shaft, a PP pinion meshes with a steel gear and idler motor which connects the steel gear shaft via a belt and applies resistance torque to the system. This motor simulates a load on the polymer gear. The wear-testing machine setup can be seen in **Figure 1**. The source motor is a GAMAK-type M21D single-phase asynchronous motor, operating at 1400 RPM and with a torque of 2.52 Nm. This motor is directly linked to a polymer gear shaft via a belt of a ratio 1:1. As for the idler motor, it is Ahmed Daoud Group Motor, with a locked rotor torque of 1 Nm. Further details and specifications can be found in the following **Table 2**.

It is worth noting that the continuous operation of gear pair engagement leads to an increase in the temperature of the gears. This temperature increase causes material expansion, especially PP pinion. To prevent this expansion from affecting the engagement of PP pinion to its shaft, a woodruff shaft key was inserted to assure a complete appendage between the pinion and the shaft.

Table 2. Specifications of the source motor [28].

Model	**GAMAK type M21D 71 M 4d**
Rated output (kW)	0.37
Rated speed (RPM)	1400
Rated torque (Nm)	2.52
Rated current (A)	3.2
Efficiency	60%
Moment of inertia (Kg.m^2)	0.0056
Locked rotor torque (Nm)	1.1
Power Factor (cos φ)	0.88

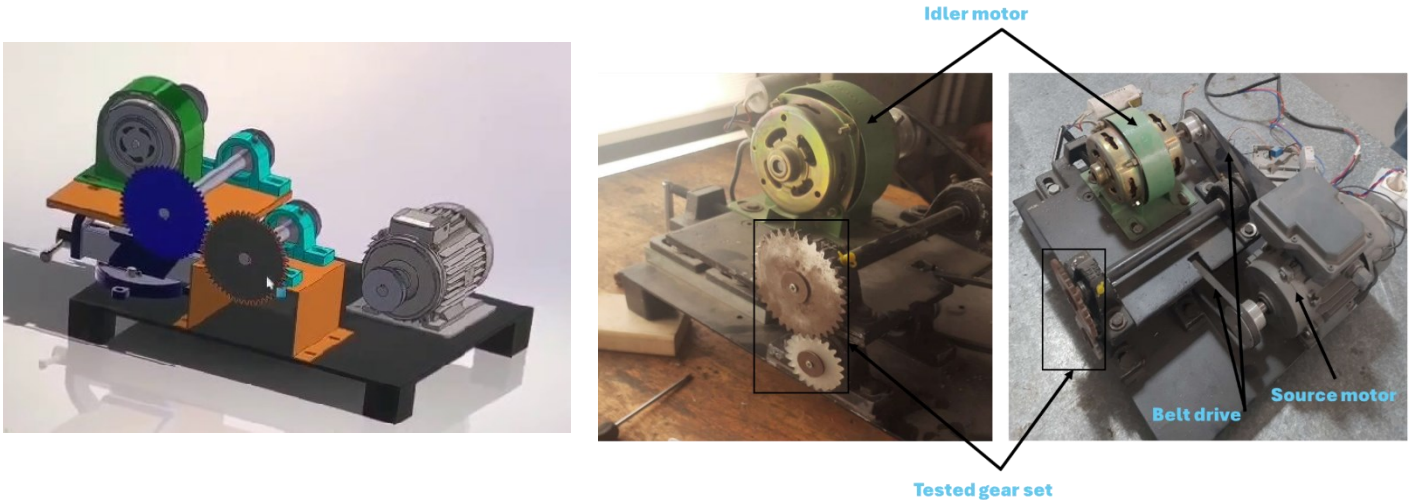

(a) 3D modelling. **(b)** Manufactured machine.

Figure 1. Wear testing machine set up.

2.3. Image and temperature capturing equipment

Using a high-quality digital camera directly correlates with the result accuracy and precise outcomes. It is essential to comprise a camera containing more pixels and high resolution to precisely capture the gear tooth. In this study, the digital camera used is Sony 12 Mega pixel with a resolution of 3024 × 4032 with f/1.8 and f/2.8 apertures, and optical image stabilization. The camera was fixed on a L-Shape bracket attached to the base of the testing machine and focused on the remarked tooth for measurements at a distance of 50 mm. For more test consistency the camera was secured to be stationary from the moment of mounting the gears on the testing machine, passing through capturing the initial pre-wear image till the final image after the machine has ceased to operate. The camera was connected to Arduino board and the figures captured were directly transformed into a Computer. It should be noted that images were captured intermittently swiftly to avoid losing temperature influence on the polymer gear tooth as the flank cools immediately after stopping the test as mentioned in previous studies. As the temperature affects the polymer gears, it was essential to estimate the pinion tooth temperature during the operation to study its effect alongside the wear of the pinion tooth. An infrared thermometer was used to

estimate pinion tooth temperature during the meshing. The thermometer used is handheld no contact Bosh model number GIS500. This thermometer offers a temperature range of −30 ℃ to 500 ℃, ensuring accurate temperature readings at image intervals.

2.4. Gear pair testing

Setting up the wear test machine, image and temperature capturing equipment, the machine operated continually for 5 hours, punctuated by an image capture at the 2nd-hour mark. A specific pinion tooth was defined by a small scratch on the pinion body as it is not certain that all teeth will wear the same way as each other. By defining the pinon tooth, one could not lose track of it at any point when the image was taken (see **Figure 2**).

(a) 0 hours. **(b)** 2 hours. **(c)** 5 hours.

Figure 2. Resulting images of the gear tooth with time interval.

Temperature readings of the specified pinion tooth were recorded at each interval of the operation alongside captured images (refer to **Table 3**). These Images served as input for image processing code calculating the wear percentage resulting from the test.

Table 3. Temperature of plastic pinion tooth in hourly intervals.

Time (hours)	Temperature (℃)
0 (pre-wear)	34.3
1	37.2
2	38.8
3	40.6
4	41
5	43.1

2.5. Image processing code

2.5.1. Preliminary image editing

To ensure no interference between steel and polymer gear teeth which may lead to inaccuracies in the wear comparison along the time intervals, preliminary editing to

crop the defined pinion tooth was required in addition to removing steel gear teeth from the cropped image (polymer gear tooth was the target image for estimating wear), thus facilitating an accurate wear comparison. This editing was done by using GUN Image Manipulation Program (GIMP). The image was cropped to a resolution of 1000 × 1000 pixels to maintain accuracy and consistency in the editing process. This resolution was selected to include the entire tooth from the dedendum to the very top of the tooth as can be seen in **Figure 3**.

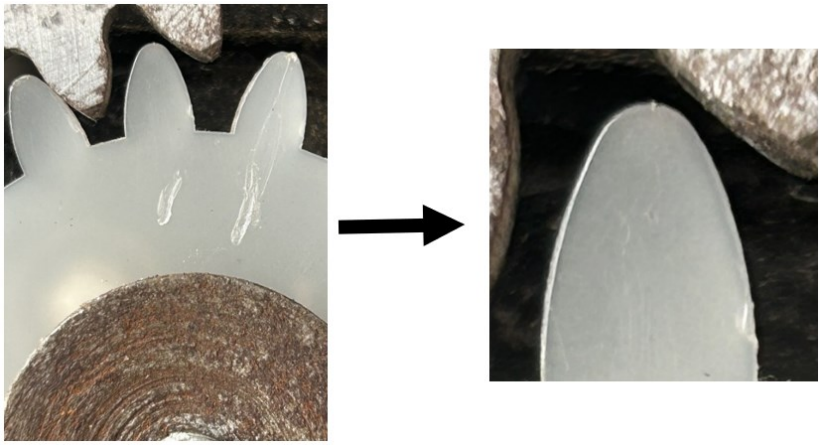

Figure 3. Cropping of the pre-wear image (0 hours).

By using a clone tool in GIMP, the steel gear teeth could be excluded from the cropped image. GIMP allows for selective copying and cloning of an image using a brush tool. **Figure 4** shows how effectively the steel gear teeth have been diminished from the cropped image, leaving the isolated polymer gear tooth for further processing. Despite the background not being a uniform solid colour due to the machine body, this minor variation shouldn't pose an issue. The detection code is designed to filter out background noise, focusing solely on selecting the profile of the plastic gear tooth, ensuring accurate analysis.

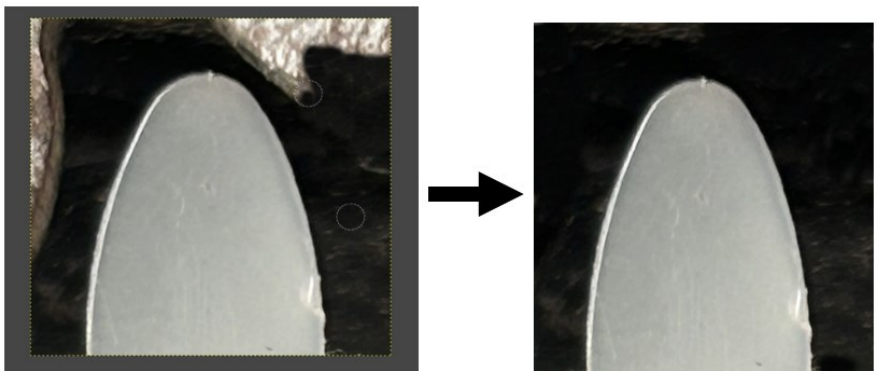

Figure 4. Usage of clone tool on steel gear (left) and pre-wear image post-editing (right).

2.5.2. Detection code

Following the preliminary editing, the edited images will be fed into the detection code, tasked with isolating the plastic gear tooth from the background. The code will then generate a binary mask, also known as a truth mask, of the gear tooth profile. In

this mask, pixels corresponding to the detected object will be turned white (with a value of 1), while all other pixels will be rendered black (with a value of 0), effectively excluding them from further analysis.

This process ensures accurate delineation of the gear tooth for subsequent processing steps. The code is implemented in MATLAB, leveraging functions from the image processing toolbox. This toolbox is renowned for its extensive collection of functions dedicated to image processing algorithms and is typically pre-installed with MATLAB due to its widespread use and popularity among researchers and practitioners. The code commences by reading the edited image of the plastic gear tooth, labelled "PP 0 plastic.jpg". In this nomenclature, 'PP' signifies the material, '0' indicates the testing hour (in this case, the pre-wear image), and 'plastic' denotes the image post-editing, indicating that the steel gear's teeth have been removed. Once the image is retrieved from the computer, it undergoes conversion to grayscale. This conversion eliminates colour information, transforming the image into a 2D matrix with dimensions of 1000 × 1000, representing the pixels with values depending on how bright or dark they are. This grayscale conversion streamlines image processing and facilitates the application of techniques such as binary masking and morphological operations (see **Figure 5**). The demonstrated code can be seen in Appendix A.

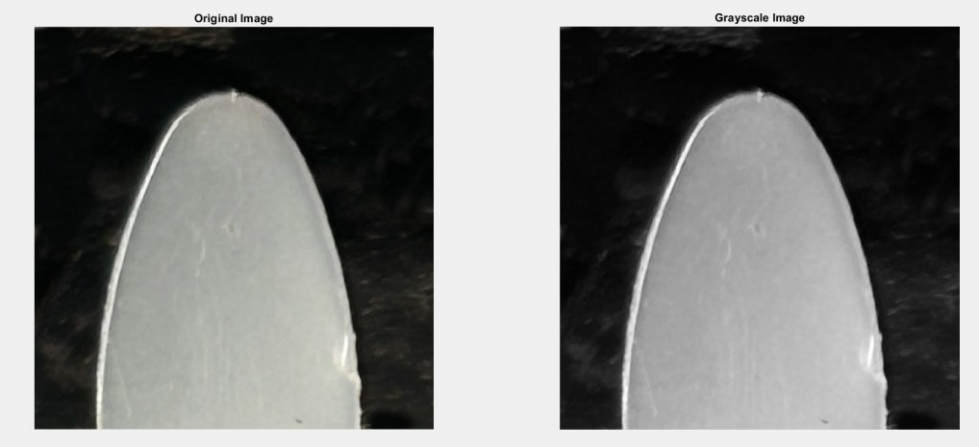

Figure 5. Grayscaling of the gear tooth image.

Following grayscaling, the image undergoes a binary thresholding process. During this process, a threshold value is established, dictating which parts of the image will become white pixels (value 1) and which will become black pixels (value 0). If a grayscale pixel's value exceeds the threshold, it is rendered as white; otherwise, it is rendered as black. It's essential to note that setting a threshold too high may only render the brightest parts of the object visible. Therefore, the threshold value, in this case set at 178, can be adjusted to accommodate different gear images based on the brightness or darkness of the gear tooth. This transformation converts the image from a 1000 × 1000 matrix with pixels of varying values into a 1000 × 1000 matrix of logical values (black 0 or white 1) as demonstrated in **Figure 6**. As depicted in **Figures 6** and **7**, the noise removal step didn't noticeably affect the image since the binary thresholding effectively addressed the background. However, this technique could prove beneficial for images where the background is brighter and inadvertently

captured during thresholding. The primary issue lies in the gaps within the gear tooth profile that haven't been accurately detected.

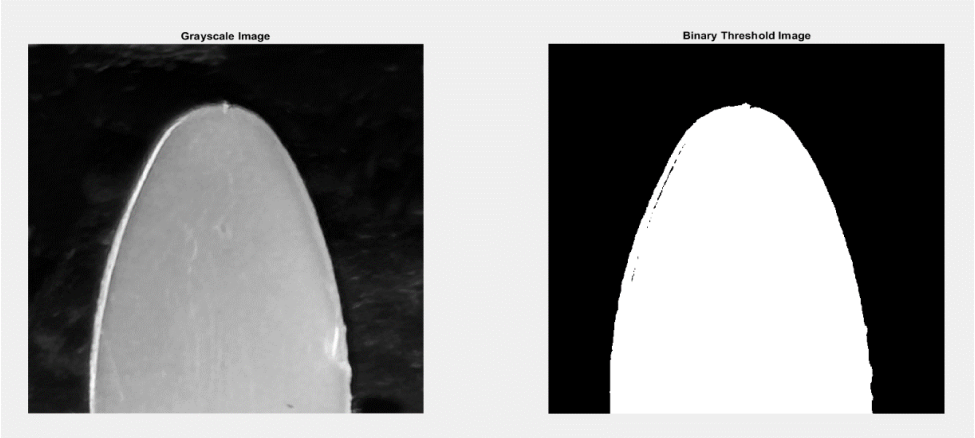

Figure 6. Binary thresholding process of the gear tooth image.

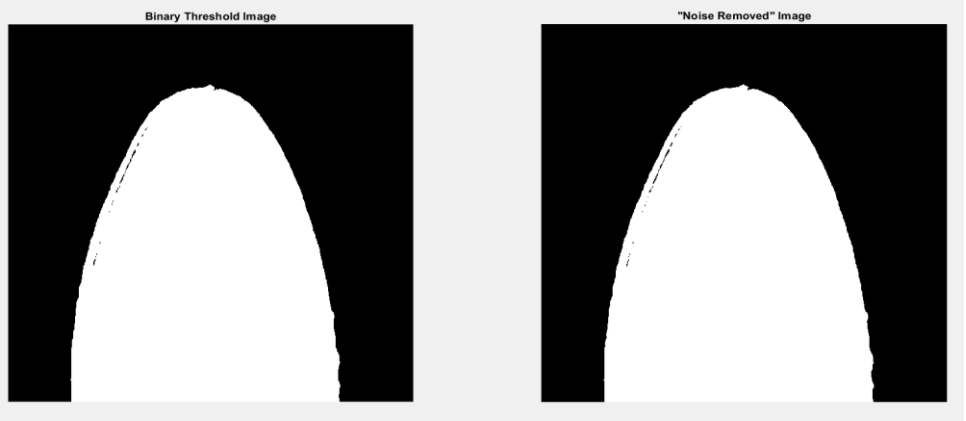

Figure 7. Noise removal in the gear tooth image.

Several solutions can rectify this issue, one of the methods, as employed in this case, is using the 'imfill' function. This function fills in any gaps or holes in image regions, effectively addressing the specific problem of incomplete detection within the gear tooth profile (see **Figure 8**).

To enhance the gear tooth profile, morphological operations are performed in **Figure 9**. A morphological operation involves creating and defining a structuring element to span the object, then joining these structural elements together using the 'imclose' function. The structuring element used in this code was a disk-shaped structure of radius 20 pixels. By applying that to the gear tooth image, the profile is enhanced to be akin to the original.

Following the morphological operation, the outcomes are visualized by displaying the original image alongside the isolated gear tooth profile. Additionally, the resulting binary image is saved on the computer. It bears the same name as the original image, except 'iso' replacing 'plastic' in the filename. This alteration underscores that the saved image represents the isolated binary mask version of that image as shown in **Figure 10**. With the detection code done, its processes are repeated for the 2-hour image and the final 5-hour image. The resulting isolated binary masks are then used as input for the wear percentage code.

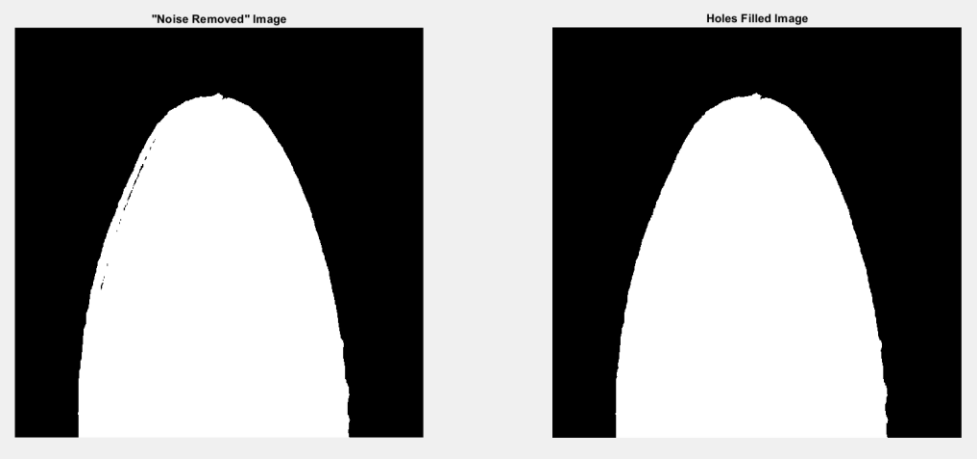

Figure 8. Gap filling the gear tooth image.

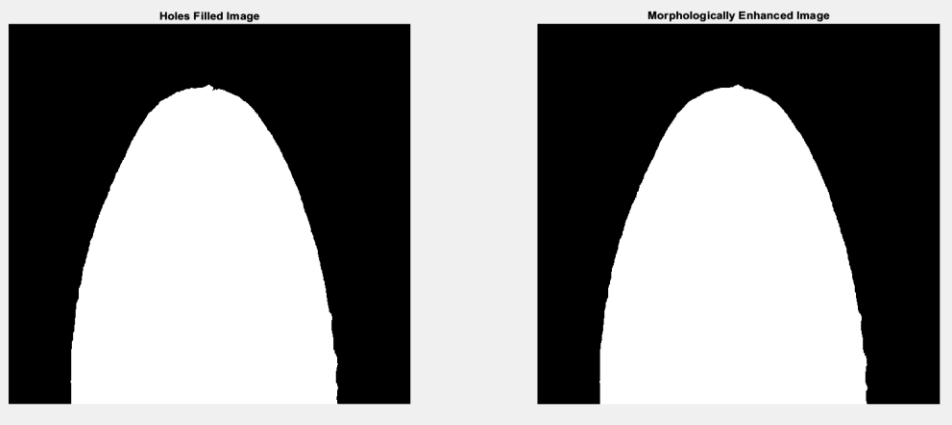

Figure 9. Morphologically enhancing the gear tooth image.

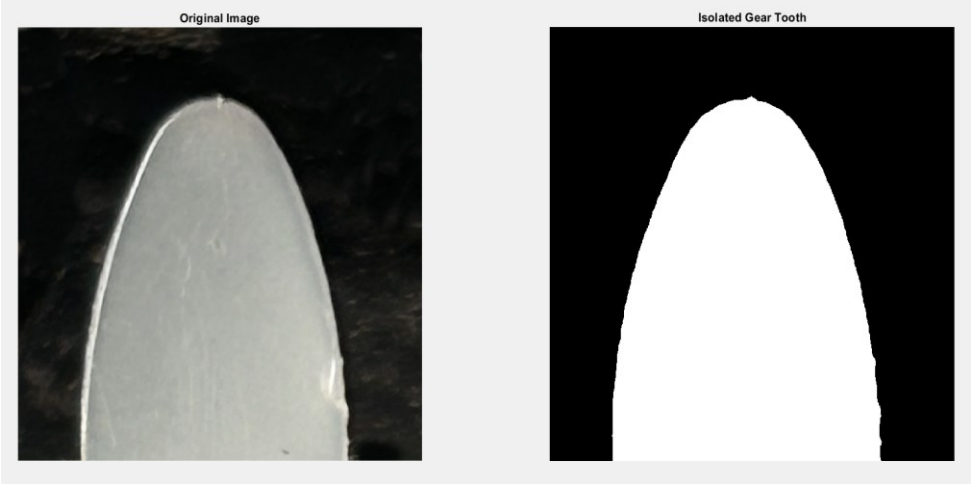

Figure 10. Output of the detection code.

2.5.3. Wear percentage calculation

The wear percentage code is designed to compute the percentage of wear on the gear tooth relative to the pre-wear image. Since all the images captured during testing undergo the same parameters of distance, angle, and zoom level, and are cropped to the same resolution without compromising quality, and processed using the same

detection code, they are effectively standardized. This ensures uniform positioning and processing of all images. Consequently, determining the wear percentage becomes straightforward. It involves counting all the white pixels in each image, subtracting the values from the pre-wear image, and then dividing by the pre-wear value to obtain the percentage of wear (wear percentage code is presented in the Appendix B) as shown by the following Equation (1).

$$W(\%) = \frac{No.of\ white\ pixels\ prewear - No.of\ white\ pixels\ worn}{No.of\ white\ pixles\ prewear} \times 100 \quad (1)$$

The wear percentage code being applied to an example binary masked gear tooth image isn't related to the test subject used in the materials and methods section, as this serves as an arbitrary example. The results of that test subject are displayed in the results and discussion section.

3. Results and discussion

Throughout the experimentation process, a systematic approach was adopted to capture images of the plastic gear tooth at regular intervals during testing. These images were subsequently processed using the detection code, which isolated the gear tooth profile and facilitated wear analysis. Upon completion of the experimentation phase and implementation of the detection code on all images, a comprehensive analysis was conducted to assess wear progression over time. The wear percentage was calculated for each image relative to the pre-wear image, providing insights into the extent of wear experienced by the gear tooth throughout the testing duration. The final results revealed a progressive increase in wear percentage over successive images, indicative of the cumulative effects of operational conditions on the gear tooth. Visual inspection of the images further corroborated these findings, with observable changes in wear patterns and surface characteristics.

3.1. Detection code results

Upon running the detection code, the pre-wear image served as the baseline for comparison. Subsequent images captured during the testing process were also processed using the same parameters and techniques outlined in the materials and methods section. To accurately represent the amount of testing undergone by each gear tooth image, we have adopted a nomenclature that includes both the timestamp and the number of cycles. This approach ensures consistency and uniformity in measuring the testing duration, accounting for potential variations in machine RPM and testing time between different tests.

The number of cycles for each image can be calculated using the following Equation (2).

$$No.of\ cycles = Time\ (mins)\ x\ input\ speed\ (RPM) \quad (2)$$

The previous equation provides a standardized metric for quantifying the testing duration and accurately tracking the wear progression of the gear tooth over time. Utilizing this equation and given that the machine operated at 1400 RPM as detailed in the materials and methods section, 2 hours give 168,000 cycles, and 5 hours give 420,000 cycles. **Figure 11** shows the zero hours (pre-wear) where it's evident that the

gear tooth profile exhibits some imperfections, particularly noticeable at the bottom right side and the top of the tooth, even before wear occurs. These nuances and imperfections may stem from manufacturing processes, such as excessive grinding during polishing, which can introduce irregularities in the gear tooth surface.

Figure 11. Detection code output for pre-wear image.

However, it's crucial to note that these imperfections in the baseline reference do not adversely affect the performance of the detection code. Since this image serves as the baseline reference for wear analysis, any wear incurred during testing will further diminish and alter the tooth profile, regardless of the initial imperfections.

After 168,000 cycles, the second picture was taken and has been run through preliminary editing and the detection code, displaying the following **Figure 12**. This figure highlights a noticeable visual disparity between the pre-wear image and the image captured after 2 hours of testing. For instance, the absence of the small chip at the top of the gear tooth in the latter image suggests that wear has occurred, resulting in the alteration or removal of this feature. Additionally, subtle changes in the profile of the gear tooth, particularly on the right side, further indicate the occurrence of wear in that region. At a total of 420,000 cycles, the final image was captured and run through the detection code, displaying the following **Figure 12**.

Figure 13 illustrates the continued evolution in the gear tooth profile, indicating further wear progression compared to the previous image. Notably, additional wear is evident around the top portion of the gear tooth, suggesting ongoing degradation in this area. Furthermore, the profile changes observed on the right and bottom-left sides of the gear tooth indicate continued alterations to the surface characteristics, possibly due to the accumulation of wear-induced damage.

Indeed, a careful examination of all the images reveals that significant deformation has not occurred in the gear tooth. If deformation had taken place, it would likely manifest as a noticeable angular displacement from the start of the dedendum, particularly indicating high-temperature deformation. The absence of such angular displacement across the images underscores the importance of conducting a thorough study of the images after processing them through the detection code. Beyond simple wear, it's crucial to scrutinize the images for any signs of deformation, such as distortion, warping, or irregularities in the gear tooth profile. These indicators

can provide valuable insights into the performance and integrity of the gear tooth under varying operational conditions.

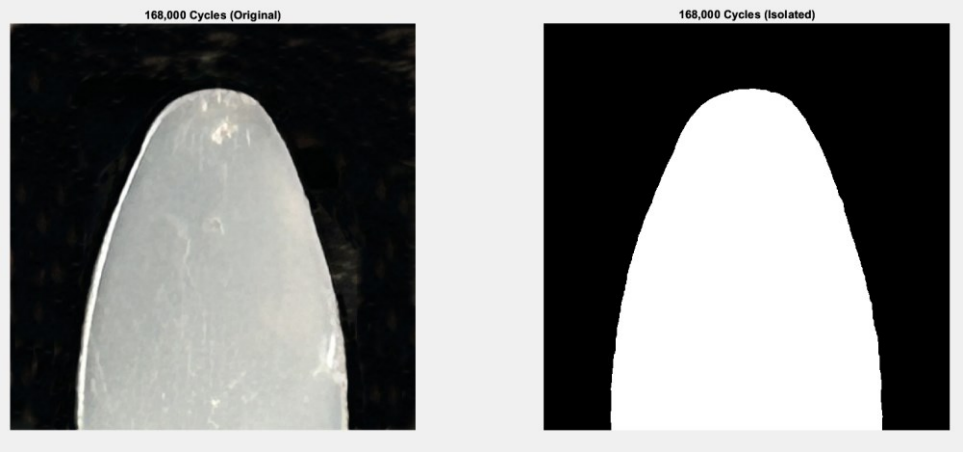

Figure12. Detection code output for 2-hour gear tooth image.

Figure 13. Detection code output for 5-hour gear tooth image.

3.2. Polymer gear wear estimation code

In this section, a quantitative analysis provided a numerical measure of the extent of wear experienced by the gear tooth over time, complementing the visual observations discussed previously. Using the wear percentage code, wear percentages were calculated as mentioned before by comparing the number of white pixels in each image to those in the pre-wear image. This comparison enables us to quantify the relative change in the exposed surface area of the gear tooth due to wear.

With the 2-hour image rendered into an isolated binary mask of the gear tooth profile, and by running the wear percentage code in comparison with the pre-wear image, the code resulted in a wear of 0.2%. This is presented in **Figure 14**. While the 5-hour image has undergone the detection code, it was inputted into the wear percentage code in comparison to the pre-wear image, displaying the following **Figure 15** with approximately 2.5% of a worn tooth. The close correspondence between visual and numerical analyses enhances our confidence in the results and underscores the importance of employing a multi-faceted approach to wear assessment.

Figure 14. Pre-wear and 2-hour image wear percentage output.

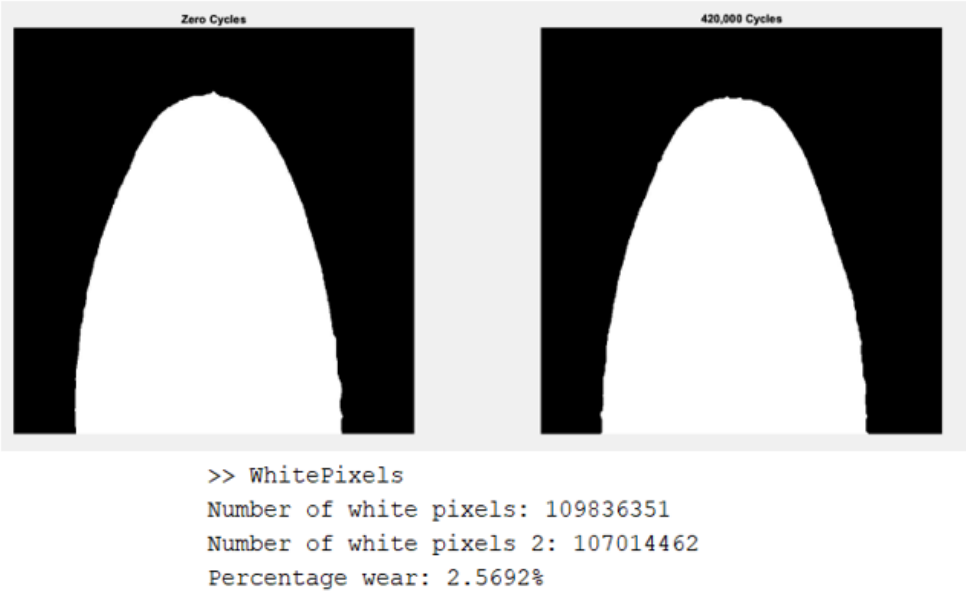

Figure 15. Pre-wear and 5-hour image wear percentage output.

3.3. Data compilation

Figure 16 represents a graph illustrating the wear percentage data collected previously. In this graph, the pointing triangles represent the experimental data points, providing a visual representation of wear progression over time. Additionally, the red solid curve depicts a cubic interpolation of the data, which attempts to interpolate the wear percentage values into a non-linear function.

The use of cubic interpolation is particularly beneficial when the nature of wear progression is unknown and cannot be easily expressed as a linear equation. By utilizing cubic interpolation, we can generate a smooth curve that closely approximates the wear percentage data points, enabling us to visualize wear progression more comprehensively. This graph facilitates the visualization of wear trends and patterns over time, providing insights into the rate and magnitude of wear experienced by the gear tooth throughout the testing duration. By analysing the wear

percentage graph, researchers can identify any notable trends, anticipate potential wear-related issues, and inform future research efforts aimed at optimizing gear performance and reliability.

Figure 17 illustrates a graph of temperature data collected during operation and testing, employing the same technique of cubic interpolation used in **Figure 16**. Similar to the wear percentage graph, the red solid curve represents the cubic interpolation of the temperature data points, providing a smooth curve that captures trends and patterns in temperature variation over time. It is noted that at low temperatures (below 370 ℃) and up to (38.50 ℃), the mechanism of wear was increasing slowly and then at a higher temperature and increased number of cycles, the mechanism increased rapidly. The material used is polypropylene without any additives and expecting at elevated temperature a large decrease in hardness. Further investigation and comparison with wear equations are needed for deep research direction.

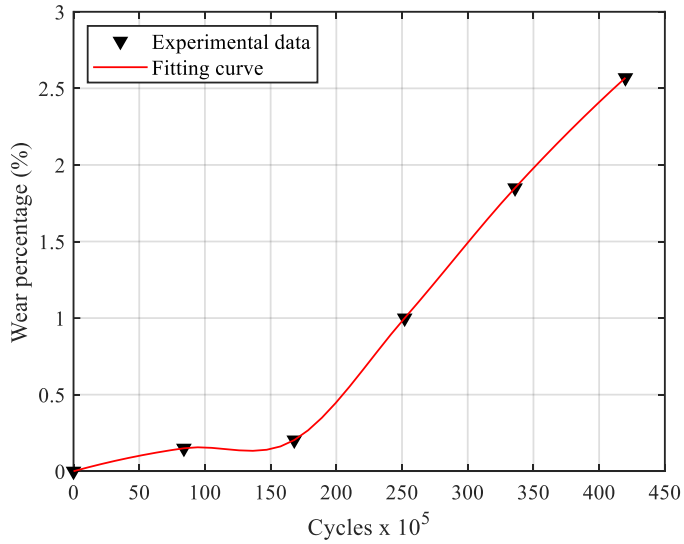

Figure 16. Wear test results for polypropylene against steel at 1.52 Nm.

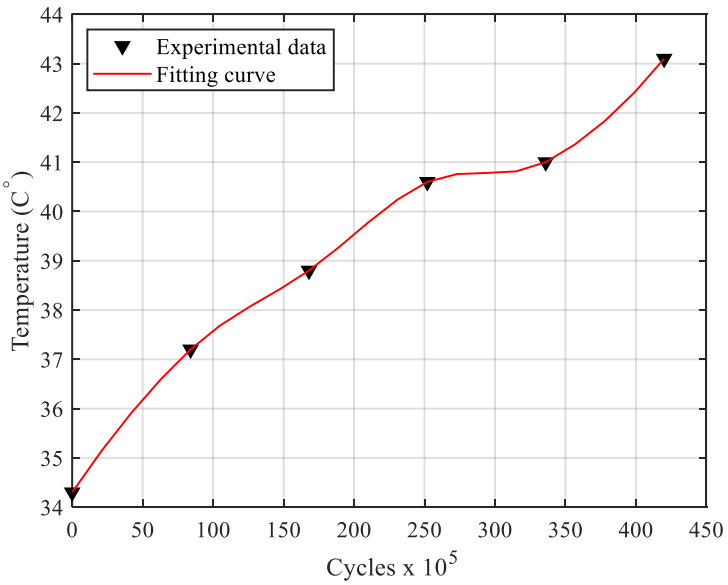

Figure 17. Temperature test results for polypropylene against steel at 1.52 Nm.

4. Conclusion

PP gear was meshed with steel gear on the wear test rig to estimate the amount of wear of the polymer gears at different cycle times. By capturing images of the PP pinion during operation at different time intervals, these images served as an input to a code for image processing to determine the amount of wear precisely without any sign of deformation. The code successfully helped in detecting the wear of the defined tooth of the PP pinion at various cycle times. Detecting tooth temperature using an infrared thermometer during the gear pair mesh assisted in accurately evaluating the tooth wear by image processing code. With this code, the wear could be detected at 2 and 5 hours with 0.2% and 2.5% respectively. It also collaborates in building graphs to explore the trends and patterns in temperature variation over time.

The paper explored avenues of assessing wear that have barely been applied in previous research papers. This research is merely the beginning of a field of gear optimization that is packed with untapped potential. With several improvements upon the methodology applied in this paper, researchers can evolve their understanding of polymers and their properties being implemented into power transmission systems. Although this novel technique succeeded in predicting the amount of wear present on the side of the gear teeth, further study needs to be conducted to predict the wear on the gear teeth flank. This technique can predict the early wear in gears while on-site without the need for disassembly. This will save time and maintenance costs, and improve the efficiency of power transmission.

Author contributions: Conceptualization, MGE and HAH; methodology, MGE and HAH; software, MGE; validation, MGE, MAE and HAH; formal analysis, MGE, MAE and HAH; investigation, MGE, MAE and HAH; resources, MGE, MAE and HAH; data curation, MGE, MAE and HAH; writing—original draft preparation, MGE, MAE and HAH; writing—review and editing, MGE, MAE and HAH; visualization, MGE, MAE and HAH; supervision, HAH. All authors have read and agreed to the published version of the manuscript.

Conflict of interest: The authors declare no conflict of interest.

References

1. Mao K, Langlois P, Hu Z, et al. The wear and thermal mechanical contact behaviour of machine cut polymer gears. Wear. 2015; 332–333: 822–826. doi: 10.1016/j.wear.2015.01.084
2. Elsiedy M, Hegazi H, Elkassas A, Zayed A. Optimum Design of Metallic and Plastic Cylindrical Gears Using Naturally-Inspired Algorithms: A Review. Journal of Engineering Research. 2023; 7(6).
3. Ignatijev A, Glodež S, Kramberger J. Computational Model for Analysing the Tooth Deflection of Polymer Gears. Polymers. 2024; 16(5): 677. doi: 10.3390/polym16050677
4. Jain M, Patil S, Ghosh SS. A review on failure characteristics of polymeric gears. In: Proceedings of the 1st international conference on advances in mechanical engineering and nanotechnology (ICAMEN 2019); 8–9 March 2019; Jaipur, India.
5. Snyder L. At the PEEK of polymer food chain. Gear Technology. 2010; 26–28.
6. Zorko D, Tavčar J, Bizjak M, et al. High cycle fatigue behaviour of autoclave-cured woven carbon fibre-reinforced polymer composite gears. Polymer Testing. 2021; 102: 107339. doi: 10.1016/j.polymertesting.2021.107339
7. Singh PK, Siddhartha, Singh AK. An investigation on the thermal and wear behavior of polymer based spur gears. Tribology International. 2018; 118: 264–272. doi: 10.1016/j.triboint.2017.10.007

8. Mao K, Greenwood D, Ramakrishnan R, et al. The wear resistance improvement of fibre reinforced polymer composite gears. Wear. 2019; 426–427: 1033–1039. doi: 10.1016/j.wear.2018.12.043
9. Elsiedy MA, Zayed AA, Hegazi HA, et al. Optimization of polyoxymethylene spur gear pair using meta-heuristic algorithms: A comparative study. Journal of Engineering Tribology. 2024; 238(9): 1153–1174. doi: 10.1177/13506501241250369
10. Elsiedy MA, Hegazi HA, El-Kassas AM, et al. Multi-objective design optimization of polymer spur gears using a hybrid approach. Journal of Engineering and Applied Science. 2024; 71(1). doi: 10.1186/s44147-024-00443-5
11. Ghazali WM, Idris DMND, Sofian AH, et al. A review on failure characteristics of polymer gear. EDP Sciences. 2017; 90: 01029. doi: 10.1051/matecconf/20179001029
12. Tunalioglu MS, Torun T. The investigation of wear on three-dimensional printed spur gears. Journal of Process Mechanical Engineering. 2021; 235(6): 2027–2034. doi: 10.1177/09544089211027732
13. Tunalioglu MS, Agca BV. Wear and Service Life of 3-D Printed Polymeric Gears. Polymers. 2022; 14(10): 2064. doi: 10.3390/polym14102064
14. Hriberšek M, Kulovec S, Ikram A, et al. Technological optimization and fatigue evaluation of carbon reinforced polyamide 3D printed gears. Heliyon. 2024; 10(13): e34037. doi: 10.1016/j.heliyon.2024.e34037
15. Muratovic E, Muminovic A, Pervan N, et al. Assessing Wear Coefficient and Predicting Surface Wear of Polymer Gears: A Practical Approach. Engineering, Technology & Applied Science Research. 2024; 14(4): 15923–15930. doi: 10.48084/etasr.7421
16. Hlebanja G, Hriberšek M, Erjavec M, et al. Durability Investigation of plastic gears. MATEC Web of Conferences. 2019; 287: 02003. doi: 10.1051/matecconf/201928702003
17. İmrek H. Performance improvement method for Nylon 6 spur gears. Tribology International. 2009; 42(3): 503–510. doi: 10.1016/j.triboint.2008.08.011
18. Mao K. A new approach for polymer composite gear design. Wear. 2007; 262(3–4): 432–441. doi: 10.1016/j.wear.2006.06.005
19. Mao K, Chetwynd DG, Millson M. A new method for testing polymer gear wear rate and performance. Polymer Testing. 2020; 82: 106323. doi: 10.1016/j.polymertesting.2019.106323
20. Mao K, Hooke CJ, Walton D. Acetal gear wear and performance prediction under unlubricated running condition. Journal of Synthetic Lubrication. 2006; 23(3): 137–152. doi: 10.1002/jsl.17
21. Mao K, Li W, Hooke CJ, et al. Polymer gear surface thermal wear and its performance prediction. Tribology International. 2010; 43(1–2): 433–439. doi: 10.1016/j.triboint.2009.07.006
22. Mao K, Langlois P, Madhav N, et al. A comparative study of polymer gears made of five materials. Gear Technology. 2019.
23. Mao K, Li W, Hooke CJ, et al. Friction and wear behaviour of acetal and nylon gears. Wear. 2009; 267(1–4): 639–645. doi: 10.1016/j.wear.2008.10.005
24. Breedsa AR, Kukureka SN, Maob K, et al. Wear behaviour of acetal gear pairs. Wear. 1993; 166: 85–91. doi: 10.1016/0043-1648(93)90282-Q
25. Kukureka SN, Chen YK, Hooke CJ, Liao P. The wear mechanisms of acetal in unlubricated rolling-sliding contact. Wear. 1995; 185: 1–8. doi: 10.1016/0043-1648(94)06575-6
26. Li W, Wood A, Weidig R, et al. An investigation on the wear behaviour of dissimilar polymer gear engagements. Wear. 2011; 271(9–10): 2176–2183. doi: 10.1016/j.wear.2010.11.019
27. Xu X, Gao F, Lopera Valle A, et al. Wear Performance of Commercial Polyoxymethylene Copolymer and Homopolymer Injection Moulded Gears. Tribology in Industry. 2021; 43(4): 561–573. doi: 10.24874/ti.1039.01.21.04
28. Zorko D, Demšar I, Tavčar J. An investigation on the potential of bio-based polymers for use in polymer gear transmissions. Polymer Testing. 2021; 93: 106994. doi: 10.1016/j.polymertesting.2020.106994
29. Johnney MA, Kumar P, Senthilvelan S. The effect of the mating gear surface over the durability of injection-molded polypropylene spur gears. Journal of Engineering Tribology. 2016; 230(12): 1401–1414. doi: 10.1177/1350650116635423
30. Černe B, Petkovšek M. High-speed camera-based optical measurement methods for in-mesh tooth deflection analysis of thermoplastic spur gears. Materials & Design. 2022; 223: 111184. doi: 10.1016/j.matdes.2022.111184
31. Soudmand BH, Shelesh-Nezhad K. Study on the gear performance of polymer-clay nanocomposites by applying step and constant loading schemes and image analysis. Wear. 2020; 458–459: 203412. doi: 10.1016/j.wear.2020.203412

32. Bravo A, Koffi D, Toubal L, et al. Life and damage mode modeling applied to plastic gears. Engineering Failure Analysis. 2015; 58: 113–133. doi: 10.1016/j.engfailanal.2015.08.040
33. Zaamout M. The Wear Behaviour of Nylon 66 and its Composites under Impact Loading. Journal of King Abdulaziz University-Engineering Sciences. 2005; 16(1): 79–95. doi: 10.4197/eng.16-1.6
34. Mertens AJ, Senthilvelan S. Mechanical and tribological properties of carbon nanotube reinforced polypropylene composites. Journal of Materials: Design and Applications. 2016; 232(8): 669–680. doi: 10.1177/1464420716642620

Appendix A

```
% Read the image
originalImage = imread('PP 0 plastic.jpg');

% Convert to grayscale
grayImage = rgb2gray(originalImage);

% Thresholding to separate the gear tooth
binaryImage = grayImage > 178;

% Remove small objects/noise
binaryImage = bwareaopen(binaryImage, 100);

% Fill holes in the binary image
binaryImage = imfill(binaryImage, 'holes');

% Morphological operations to enhance the gear tooth
se = strel('disk', 20); % Define a disk-shaped structuring element
binaryImage = imclose(binaryImage, se);

% Display the results
figure;
subplot(1, 2, 1);
imshow(originalImage);
title('Original Image');
subplot(1, 2, 2);
imshow(binaryImage);
title('Isolated Gear Tooth');

% Save the isolated gear tooth image
imwrite(binaryImage, 'PP 0 iso.jpg');

```

Figure A1. MATLAB gear tooth detection code.

Appendix B

```
% Read the image
binary_img = imread('PP 0 iso.jpg');

% Count the number of white pixels (pixels with value 1)
num_white_pixels = sum(binary_img(:));

% Display the number of white pixels
disp(['Number of white pixels: ', num2str(num_white_pixels)]);

% Read the 2nd image
binary_img2 = imread('PP 2 iso.jpg');

% Count the number of white pixels (pixels with value 1)
num_white_pixels2 = sum(binary_img2(:));

% Display both images
figure;
subplot(1, 2, 1);
imshow(binary_img);
title('Initial');
subplot(1, 2, 2);
imshow(binary_img2);
title('2 hours');

% Display the number of white pixels
disp(['Number of white pixels 2: ', num2str(num_white_pixels2)]);

% Calculate and display the wear percentage
percent_wear = ((num_white_pixels - num_white_pixels2)/num_white_pixels)*100;
disp(['Percentage wear: ', num2str(percent_wear), '%']);
```

Figure B1. Wear percentage code.